Evidence for narrow dibaryons at 2050, 2122, and 2150 MeV observed in inelastic pp scattering

B. Tatischeff,[1] J. Yonnet,[1] M. Boivin,[2] M. P. Comets,[1] P. Courtat,[1] R. Gacougnolle,[1] Y. Le Bornec,[1] E. Loireleux,[1] F. Reide,[1] and N. Willis[1]

[1]*Institut de Physique Nucléaire, CNRS/IN2P3, F-91406 Orsay Cedex, France*

[2]*Laboratoire National Saturne, CNRS/IN2P3, F-91191 Gif-sur-Yvette Cedex, France*

(Received 1 October 1998)

The reaction $pp \Rightarrow p\pi^+X$ was studied in order to look for dibaryons at invariant masses M_{pX}. The experiment was performed at three different energies ($T_p=1520$, 1805, and 2100 MeV) and at several different angles from 0° up to 17° (lab). Narrow dibaryons were observed in invariant mass spectra at 2050, 2122, and 2150 MeV. The corresponding numbers of standard deviations vary between 3.2 and 12.6. The mass of these narrow dibaryons agree with systematic studies of dibaryonic masses experimentally observed through many experiments performed by various collaborations. Such a systematic study allows us to define the mean dibaryonic mass spectrum, and is found to be in agreement with the spectrum calculated within a simple phenomenological mass formula based on color magnetic interactions between two colored quark clusters. [S0556-2813(99)03204-5]

PACS number(s): 14.20.Pt, 13.75.−n, 12.40.Yx

I. INTRODUCTION

The experimental search for narrow dibaryons is an essential task for several reasons. Such dibaryons, if their existence is confirmed, are a crucial argument to decide whether or not physics at a few GeV can be entirely explained by baryonic and mesonic degrees of freedom or if additional assumptions such as quark degrees of freedom, must also be considered. Over the past 20 years, many results have been obtained from experiments (not always carried out with the highest precision) that have led some authors to conclude that they have observed such structures—whereas others reach the contrary conclusion. It is therefore highly desirable to reach a conclusion concerning the existence of these narrow dibaryons, regardless of their origin.

The main reason for the unceasing debates related to the existence of narrow dibaryons is the weakness of their signatures compared to the superimposed physical background of baryons and mesons in interaction for masses larger than the pion production threshold mass (2014 MeV). For these studies, the useful experiments needed to be as precise as possible.

Such a precise experiment was performed using a proton beam. The reaction $pp \Rightarrow p\pi^+X$ was studied in order to look for the dibaryonic M_{pX} invariant mass simultaneously with the study of the missing mass M_X (whose results were presented elsewhere [1,2]). Here the missing mass can be either one neutron (exclusive measurement), or $N\pi$. The experiment will be described in the next paragraph. The results will then be presented and discussed. A review of the results from several experiments studied previously will be presented. Finally, an attempt to interpret these results will be presented, followed by a discussion describing other possible interpretations.

II. EXPERIMENT

The experiment was performed at the Saturne synchrotron beam facility using the SPES3 system (see Fig. 1). The beam energies were 1520, 1805, and 2100 MeV. The beam flux varied between 10^8/burst and 5×10^8/burst, depending on the spectrometer angle (and incident energy), in order to keep the acquisition dead time to less than 10%. The liquid H_2 target of 393 mg/cm^2 was held in a container with 130 μm thick Ti windows. External heat shields comprised of 24 μm thick aluminum were placed in the beam-line on either side of the target.

The SPES3 spectrometer properties are described elsewhere [3,4]. To summarize its main properties, it is a mean value solid angle spectrometer (± 50 mrd in both the horizontal and vertical planes), and secondly that it is a large momentum range spectrometer ($600<pc<1400$ MeV). Both particles were detected in the same setup consisting of several drift chambers. The information from these detectors was used to reconstruct the particle trajectories. The first chamber C1 (MIT-type), was situated on the spectrometer focal plane. Its spatial and angular horizontal resolutions

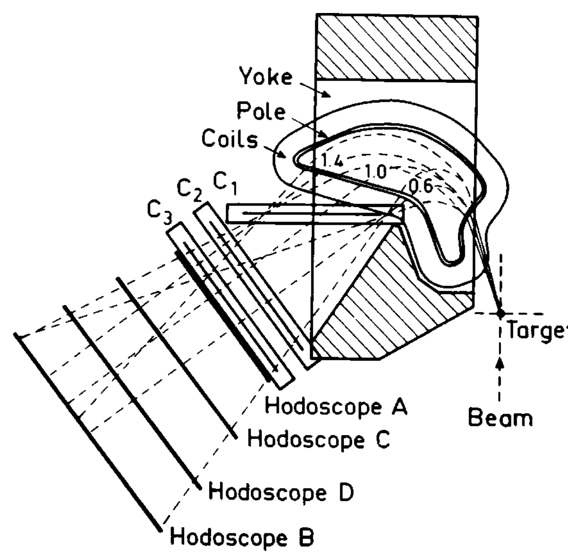

FIG. 1. The SPES3 spectrometer and the associated detection system.

were $\sigma_x = 90$ μm and $\sigma_\theta = 18$ mrd, respectively. Two multidrift chambers, C2-C3, or CERN chambers, which were perpendicular to the mean particle direction were designed to get information on trajectories in the horizontal and vertical planes. But, due to the small vertical magnification of the spectrometer (≈ 0.14), the ϕ resolution at the target was too poor to be useful. Nevertheless, these CERN chambers were used to determine the MIT chamber efficiency by calculating the ratio of three to two counterhits. During the experiment, the maximum value was 96% and the variation of this efficiency was monotonous along the focal plane (without any discontinuity).

The trigger consisted of four planes of plastic scintillator hodoscopes. The dimensions of each plastic detector were 12×40 cm^2 for the first plane (A), and 18×80 cm^2 for the last plane (B). Each of these two planes were comprised of 20 scintillators. The time of flight baseline from the first scintillator plane to the last scintillator plane was 3 m. Particles were identified by their time of flight between the A_i and B_j detectors and also by their energy loss in the A_i detectors. This latter measurement was mainly used to discriminate between one and two charged particles. Meantimers and constant fraction discriminators were used and the time resolution for each scintillator was typically $\sigma = 180$ ps. The large horizontal angular magnification of the spectrometer produced a large horizontal angular opening (up to 30°) of the trajectories at the output of the spectrometer. It resulted in a large number of useful $A_i \cdot B_j$ combinations (125), between the first and last scintillation counter planes, which required the same number of coincidences. It is important to note that a mean range of 200 MeV/c (25% of the focal plane acceptance) is covered by each $A_i \cdot B_j$ combination. Therefore, there is a large overlap between many $A_i \cdot B_j$ trigger combinations for each spectrometer momentum. Moreover, when the scattering angle or the incident energy vary, this domain for a fixed $A_i \cdot B_j$ combination shifts with invariant mass M_{pX}. Careful calibrations and efficiency measurements of all the 125 combinations were performed using a system of scintillator counters moving in front of the A-hodoscope and behind the B-hodoscope. The trigger efficiency mean value is of the order of 95%.

Since both particles, p and π^+ were analyzed by the same detector elements, events were lost when both their trajectories intersected on each plane of the detection system (drift chamber or trigger hodoscope). A simulation code was written in order to correct for the loss of such events. For M_{pX} invariant masses ($M_X > M_n$) the correction function was a smooth function varying between 1.1 and 1.3. For $M_X = M_n$, the correction function was also smooth except in a narrow range of invariant masses, when both trajectories intersected on the focal plane. When such a correction creates an oscillation, as small as it may be, the corresponding data are removed, in order to avoid introducing a spurious peak due to this correction. The normalizations of the number of events, were performed using two telescopes that had a view of the target, and an ionization chamber located in front of the beam dump. The information from these detectors was normalized by ^{12}C activation measurements.

A second time of flight ($A_i \cdot A_j$) between both particles was used in order to eliminate random coincidences and possible wrong identifications coming from real $pp \to ppX$ events. A correction was made to take into account the differences in trajectory lengths, and then a common window of ± 2 ns was used for all the 190 ($19 \times 20/2$) times of flight channels gathered in Fig. 2. The resolution of this distribution is $\sigma \approx 570$ ps. When the data reduction code associated a wrong assignment of the trigger and chamber information (0.6% of events), the corresponding information was removed.

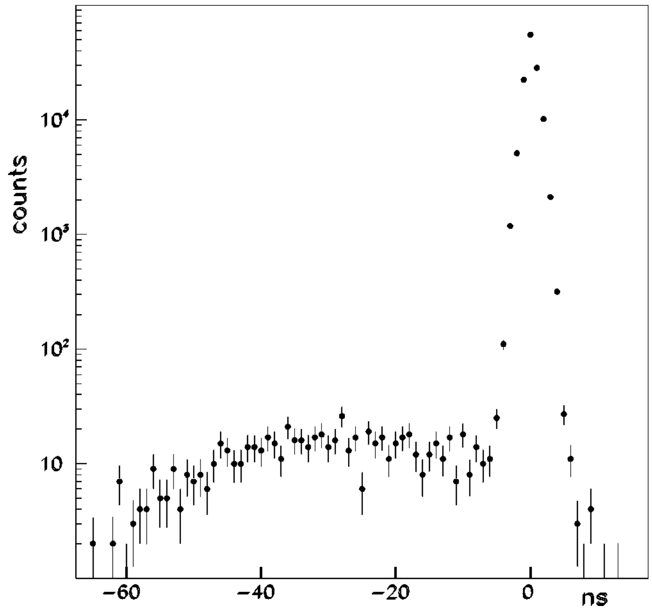

FIG. 2. Overall time of flight (log scale) of the 190 A_i-A_j combinations.

Special care was taken to ensure that no bias could be produced by particles originating from scattering on mechanical pieces at the entrance of the spectrometer. A detailed discussion of this part of the analysis was presented in Ref. [1]. The effect of the target windows was checked by regular empty target measurements. The corresponding counts were small, a few %, depending on the scattering angle and the missing mass range. We therefore deduced that the target windows were not a source of noticeable contamination. We also deduced that although our measurements were performed at small angles, the data were not contaminated by any hot area of incident beam which could have been scattered by some mechanical piece at the entrance of the spectrometer. We will quantitatively illustrate further (Sec. III B) the very small contribution of the empty target compared to the H_2 data in the M_{pX} range studied.

The raw data obtained at $T_p = 1805$ MeV, $\theta = 0.75°$ (lab) before any correction or normalization, are shown in Fig. 3. The blank line corresponds to the area where the p and π^+ momenta are the same. We observe the absence of any hot or inefficient wires which would result in an intense or light cross (horizontal and vertical lines) in the whole range of the scatter plot. The dark area corresponds to the events of the $pp \to p\pi^+ n$ reaction covering a momentum range of 500 MeV/c (900–1400 MeV/c). The corresponding missing mass spectrum presented in Fig. 4 shows a continuous distribution of the neutron peak.

A simulation code was written in order to study the consequences of particles scattered by the target in the vertical plane at angles $50 \leqslant |\phi| \leqslant 80$ mrd. No narrow structure ap-

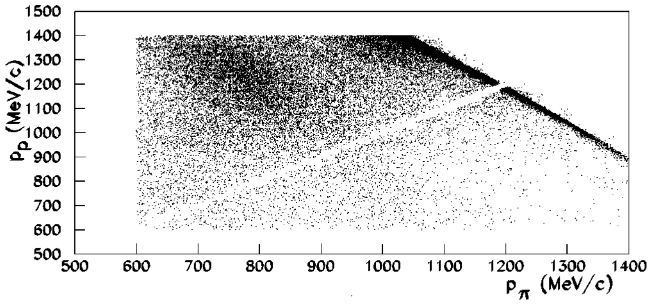

FIG. 3. Scatter plot of proton momenta versus pion momenta for events at $T_p = 1805$ MeV, $\theta = 0.75°$ lab.

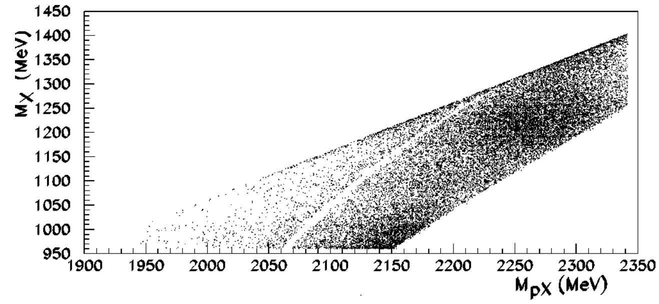

FIG. 5. Scatter plot of missing mass versus dibaryonic invariant mass events at $T_p = 1805$ MeV, $\theta = 0.75°$ lab. A cut was applied to the missing mass in order to remove the $p\pi^+n$ events.

peared in M_{pX} invariant masses which could have been attributed to such a bias.

The beam polarizations were 0.78, 0.74, and 0.70 for the three increasing energies. The polarities were reversed after each spill in order to avoid any bias due to slow polarization drift.

III. RESULTS

A. General presentation

The data shown in Fig. 3 are also presented in a scatter plot (Fig. 5) of the missing mass, M_X, versus the invariant mass, M_{pX}. In this figure several software cuts have been applied to M_X. In order to suppress the very intense line corresponding to the $p\pi^+n$ reaction, we selected events for $M_X > 960$ MeV. The blank curved line corresponds to the area where the p and π^+ momenta are the same, as previously mentioned. The external cuts are due to p and π^+ momenta limits at 600 and 1400 MeV/c, respectively. The three intense regions correspond to the following.

$M_X \approx 960$–1000 MeV and $M_{pX} \approx$ 2150 MeV. This is a remaining tail from the $pp \rightarrow \Delta^{++}n$ reaction which is insufficiently cut in this figure and will be discussed later.

$M_X \approx 1200$ MeV (Δ mass) and $M_{pX} \approx 2270$ MeV. These events correspond to the production of two deltas: Δ^{++} and Δ^0. They are not genuine broad resonances in the dibaryonic system.

The increase in intensity along the upper limit of the scatter plot is due to the nonlinear transformation between the proton momenta and the missing masses.

Different corrections and normalizations were applied, with a corresponding increase of the errors depending on the precision of the following factors: detection cell efficiencies, dead time losses, normalization of the number of events by the incident proton flux, lost events due to trajectories that intersect in one of the planes of the detection system, and normalization of the cross sections to constant momenta acceptances: Δp_p and Δp_{π^+}.

The major part of these corrections was quantitatively determined using a simulation code written for this purpose. Careful attention was paid to experimental biases which could have been produced by some discontinuity in the correction functions (last two corrections). Software cuts were introduced on M_X at a value large enough so as to avoid

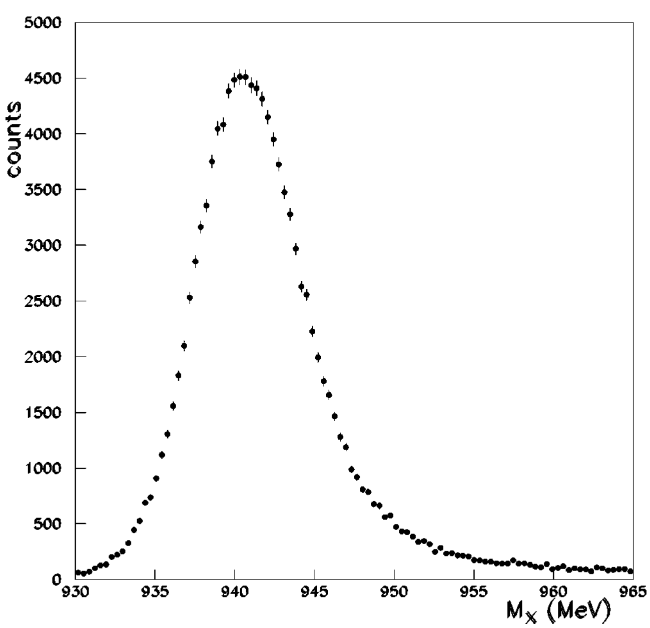

FIG. 4. Neutron missing mass peak at $T_p = 1520$ MeV, $\theta = 0°$ lab.

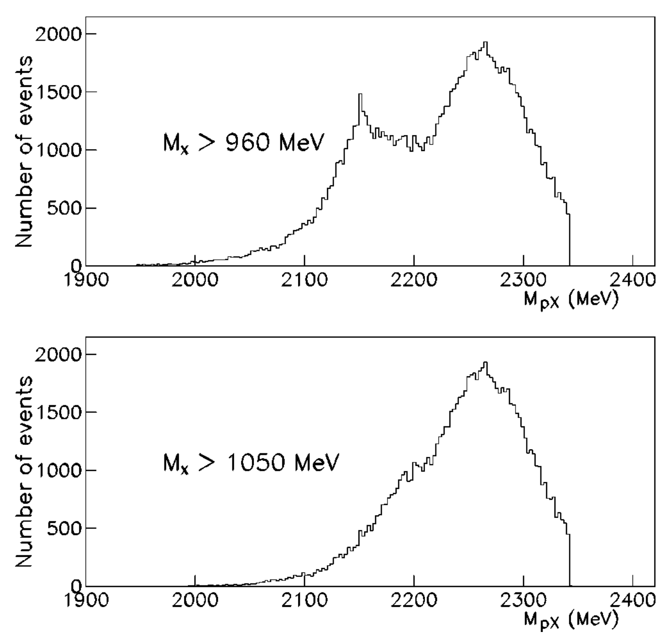

FIG. 6. Number of events for dibaryonic M_{pX} invariant mass for two different cuts on the missing mass value at $T_p = 1805$ MeV, $\theta = 0.75°$ lab.

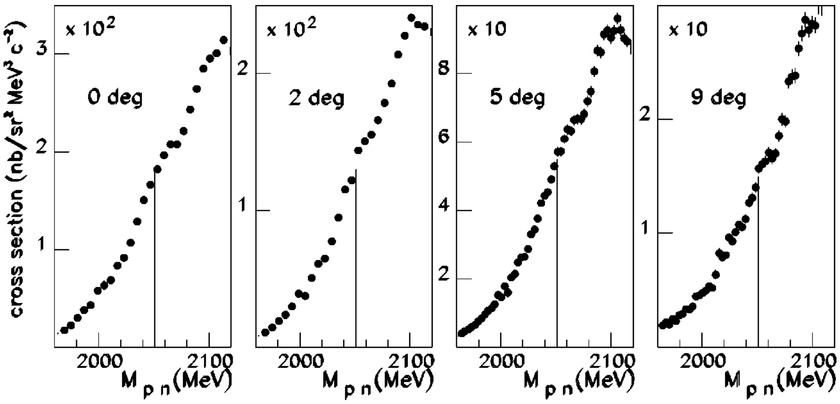

FIG. 7. Cross sections for 1520 MeV incident protons versus the M_{pn} dibaryonic mass showing a small and narrow structure around 2050 MeV.

introducing a bias due to the n missing mass tail. The effect of such cuts can be anticipated from Fig. 5 and is illustrated in Fig. 6. The upper part shows the horizontal projection of Fig. 5, with an important tail from residual $\Delta^{++}n$ reactions. There is a remaining peak which will be reduced after normalization to constant momenta, but a discontinuity will remain. This peak in dibaryonic M_{pX} masses disappears totally when a software threshold of 1050 MeV is applied to the missing mass spectra as shown in the lower part of Fig. 6.

Our experimental cuts ($600 \leqslant p \leqslant 1400$ MeV/c) remain constant, but the behavior of the range of the events studied in the $M_X = f(M_{pX})$ scatter plot (Fig. 5), changes with incident energy. The tail of the neutron missing mass decreases with increasing energy. The intense $pp \to \Delta^{++}\Delta^0$ spot seen in Fig. 5 moves inside the range and is located totally inside our range at $T_p = 1805$ MeV. Finally the empty line from $p_p = p_{\pi^+}$ momenta is less inconvenient at higher energy, since it is located in a less central position in the $M_X = f(M_{pX})$ scatter plot.

B. Results at $T_p = 1520$ MeV

In Fig. 7, we see the M_{pX} dibaryonic spectra obtained at $T_p = 1520$ MeV for neutron missing masses $930 \leqslant M_X \leqslant 960$ MeV and at all forward angles where the data were obtained with a good resolution and large statistics. At all angles, a narrow structure appears around 2050 MeV, straight lines are drawn at this value. Figure 8 shows the corresponding angular distribution of the c.m. cross section, extracted by using low order polynomials for the background and a Gaussian peak for the structure. The number of standard deviations (S.D.) vary from 12.6 at 0° up to 4.9 at 9°. The mean value of the width is $\sigma \approx 12.6$ MeV. The curve is only to guide the eye.

Statistically, this result is significant since we treated for the first angle at 0°, 126 300 events in the region of the neutron missing mass. This number reduced to 118 410 after the time of flight selection. After cuts on the M_{pn} invariant mass in the range 2030–2070 MeV, there remained 26 440 events (with a statistical precision of $6^0/_{00}$). After corrections and peak over background extraction, the final relative precision (see Fig. 8) was 7.8%. Figure 9 shows the number of events for the same data set shown in Fig. 7 at the two smallest angles (dark points). They are compared to the empty target measurements (open points). The ratio between full and empty target data is close to 180. The empty target data are presented for ten times more incident protons in order to make them visible.

For missing masses larger than the neutron mass ($M_X \geqslant 960$ MeV) other checks were performed to make sure that the corrections applied could not be a source of false structures. They are illustrated in Fig. 10 for $T_p = 1520$ MeV at 2°: the correction for lost events were made over elementary surfaces in the scatter plot $M_X = f(M_{pX})$, as opposed to mean corrections which were made on the single variable M_{pX}; a limited smooth area was arbitrarily selected in order to avoid all eventual structured cuts. Such an area is shown in part (a) of Fig. 10 between the two arcs.

The corresponding consequence on M_{pX} distribution is shown in part (b) of Fig. 10. We see a structure around 2122 MeV (↓). Then the same analysis was performed for all the events in the scatter plot. The resulting M_{pX} distribution is shown in part (c), which shows again the same structure.

We conclude that the structure around $M_{pX} = 2120$ MeV and $\theta = 2°$ is a genuine dibaryon and not an experimental artifact. On the other hand, the broad peak observed around 2170 MeV is a part of the $\Delta - \Delta$ final state.

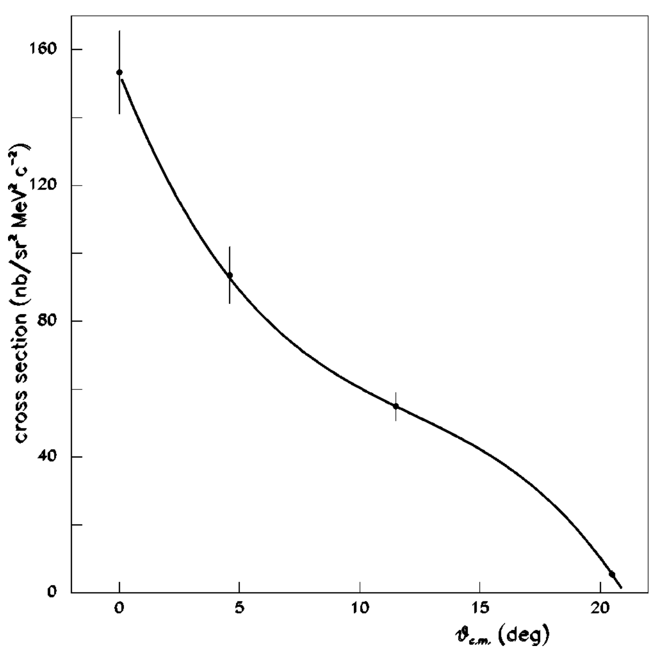

FIG. 8. Center of mass cross section of the dibaryonic structure observed at $M_{pn} = 2050$ MeV for 1520 MeV incident protons.

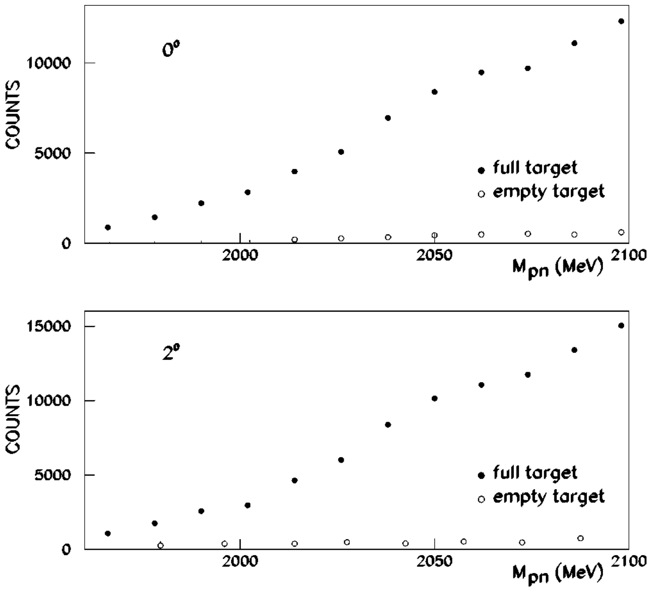

FIG. 9. Invariant mass M_{pn} spectra for full and empty target data at $T_p=1520$ MeV, $\theta=0°$ and $2°$. The empty target data were normalized to the same number of incident protons, then were multiplied by ten to make them visible.

The cross sections for M_{pX} dibaryonic invariant masses are shown in Fig. 11. The data were regrouped in order to reduce the statistical errors. The limits on M_X were adjusted in order to cut all regions having experimentally ''intense'' or ''weak'' counting areas in the $M_X=f(M_{pX})$ scatter plot. The intense counting area was produced by the tail of $p\Delta$ or $\Delta\Delta$ reactions in the final state. The weak counting area corresponds to the region where p_p and p_π momenta are closed.

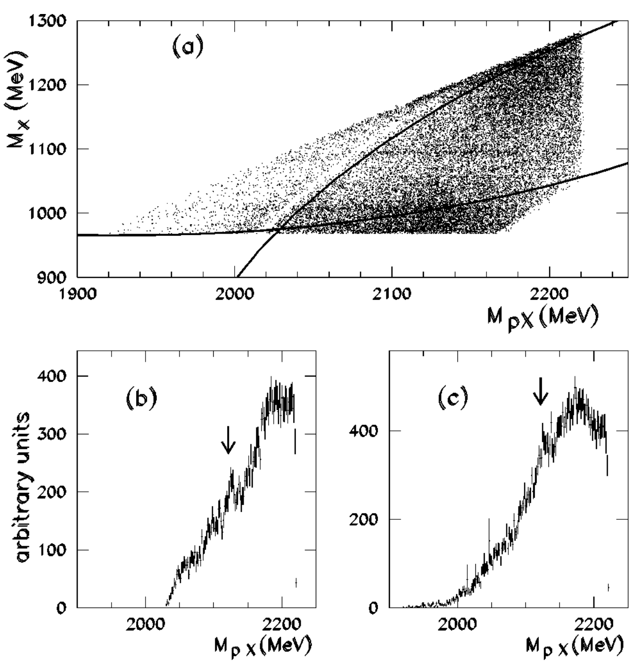

FIG. 10. For $T_p=1520$ MeV and $\theta=2°$, part (a) shows the scatter plot of the raw data, and two arcs used to define a surface where only smooth corrections were applied. Part (b) shows the resulting M_{pX} distribution (see text). Part (c) shows the M_{pX} distribution when all the data ($M_X\geqslant 960$ MeV) was considered.

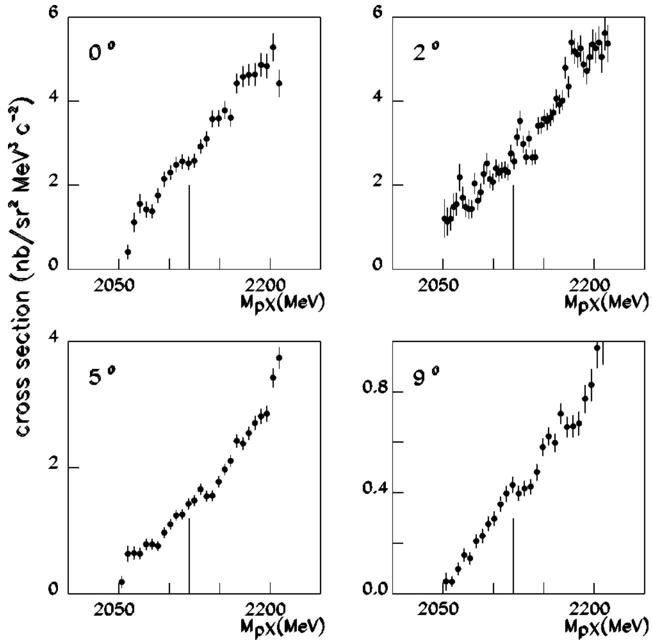

FIG. 11. Cross sections for 1520 MeV incident protons versus M_{pX} dibaryonic mass for missing masses $M_X\geqslant 960$ MeV. Straight lines are drawn at 2122 MeV.

Therefore all regions of nonsmooth corrections were eliminated. The range in M_{pX} dibaryonic mass is higher than previously discussed and does not explore the region below 2050 MeV. Also the statistics are smaller. At all forward angles, there is a structure at a mean mass value of 2122 MeV. Straight lines are drawn for this M_{pX} mass. Although these structures are seen at all four forward angles, they are not well defined and therefore no cross section extraction was performed. There are also signs of structures at 2066 MeV (2°), 2183 MeV (2°) and 2170 MeV (9°).

Since the experiment was performed using polarized proton beams, the analyzing powers were also measured. Figure 12 shows the analyzing powers for the two missing mass data, for 1520 MeV incident protons at 5 and 9 degrees, since there is no polarization for forward angles, and since the resolution and the counting rate spoil for larger angles.

Although the error bars are smaller for neutron missing mass data than for $X=N\pi$ missing mass data, there is no indication, in the analyzing power results, of any structure at the masses where they appear in the cross sections. In the case of larger missing masses $M_X>M_n$, structures can be seen (with a low confidence level).

C. Results at $T_p=1805$ MeV

Checks similar to those described for $T_p=1520$ MeV data were performed for 1805 MeV data. Inside the scatter plot $M_X=f(M_{pX})$ several selections were carried out with continuous and smooth corrections. None of them allowed us to extract a narrow and small dibaryonic structure. This is illustrated in Fig. 13 where we see that two large, broad peaks corresponding to Δn and $\Delta\Delta$ reactions dominate the cross section. The Δn tail remains in spite of the cuts introduced in order to eliminate it. Similar results were obtained at all angles between 0.75° and 13°, with the distinctive result that the ratio of Δn over background decreases with increasing

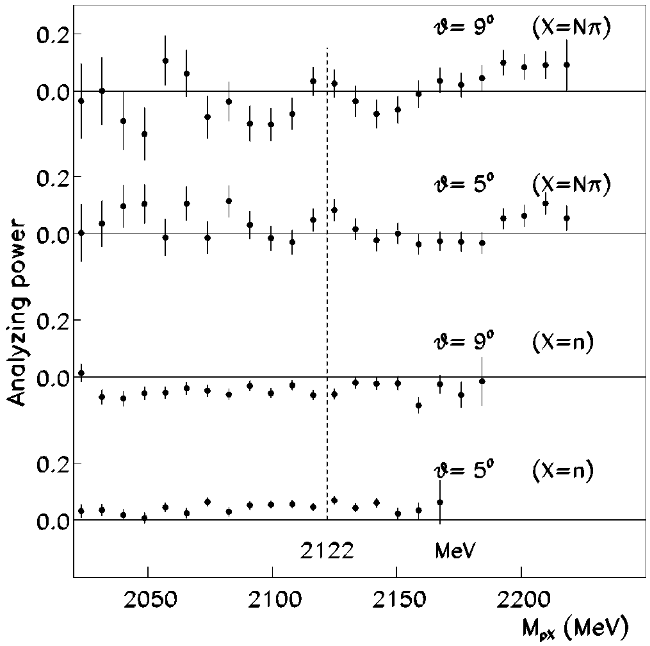

FIG. 12. Analyzing power versus M_{pX} dibaryonic masses for data at 5° and 9° and 1520 MeV incident protons.

angle. We conclude therefore that the $T_p = 1805$ MeV energy was not suited for the observation of narrow dibaryon structures with our experimental conditions.

D. Results at $T_p = 2100$ MeV

At this energy, no measurement was performed at angles larger than 9° lab. The consequence of the large number of two-delta production events observed in the missing mass M_X and invariant mass $M_{p\pi^+}$ was that in the case of the M_{pX} dibaryonic mass, a large maximum occured at around 2300 MeV (not shown).

By using appropriate cuts defining smooth boundaries in the $M_X = f(M_{pX})$ scatter plot, it was possible to extract the cross sections, presented in Fig. 14. A dibaryon at $M_{pX} = 2150$ MeV ($\sigma = 11$ MeV) was clearly extracted from polynomial background at forward angles 0.7° and 3°, with respective values of 8.1 and 5.5 numbers of S.D.'s.

An extension of the cross sections at three angles between 2170 and 2270 MeV is shown in Fig. 15. A smaller structure

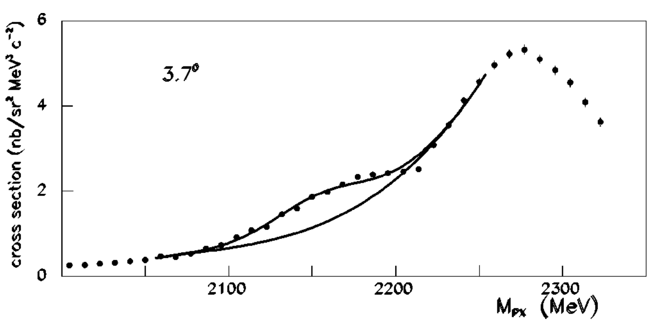

FIG. 13. Cross sections for 1805 MeV incident protons versus M_{pX} dibaryonic mass at 3.7°. Cuts were introduced in order to remove the main part of the Δn peak. However a tail remained which gave a peak around $M_{pX} = 2160$ MeV. A large $\Delta\Delta$ peak is observed around 2280 MeV.

is present at all angles around 2230 MeV. Since the corresponding S.D.'s are $\leqslant 2.6$, the existence of a dibaryon is possible but not sure.

IV. REVIEW AND DISCUSSION OF PREVIOUS RESULTS

A large number of experiments were performed in order to search for narrow dibaryons. Some of the authors have not observed them, and therefore have concluded on their nonexistence. We will focus on the results where narrow dibaryonic structures have been observed and therefore advocated. Several results were obtained from bubble-chamber slide studies. They are of course low statistics experiments. Since they were reported on different occasions [5,6], they will not be mentioned here. Our discussion therefore does not presume to be exhaustive. Some other precise experiments which will be recalled in the next paragraphs, were already mentioned previously in more detail [5,6].

The aim of the following discussion is to recall several results, preferably the most recent ones.

A. Previous precise results in the *N-N* elastic channel

1. pp elastic differential cross sections

Cross sections for pp elastic scattering were measured at COSY [7] in the range $2112 < \sqrt{s} < 2866$ MeV with bins which are equal to $\delta\sqrt{s} \sim 9.5$ MeV around $M_{pp} = 2122$ MeV. No structure was observed. The range of that study is marginal as compared to the range studied in our experiment.

2. $\vec{p}p$ elastic scattering analyzing powers

Narrow structures were observed at KEK [8,9] in the analyzing powers at the following invariant masses: 2160 MeV ($\Gamma_{1/2} = 14$ MeV) and 2192 MeV ($\Gamma_{1/2} = 13$ MeV). However very precise measurements were performed later at Saturne [10] using the SPES3 beam line and an energy degrader with variable thicknesses (rotating wheel). The large overlap between the results obtained from the Saturne experiment, for different extracted proton energies, allowed very precise relative adjustments. Such a precaution is important since the $\gamma G = 3$ depolarization resonance occurs in this energy range. No structure was observed in the data of this Saturne experiment.

B. Previous precise results in inelastic channels

1. Recall of some previous precise results concerning the dibaryon at 2122 MeV

A dibaryon was already observed at 2122 MeV from electronic and bubble chamber slide experiments. The ^{3}He$(p,d)X$ reaction was studied at the Saturne SPES1 beam line, some years ago, using electronics, therefore with good statistical precision [11,12]. The missing mass M_X had the following quantum numbers: $T_X = 1$ and $B_X = 2$. The experiment was performed at three energies: 750, 925, and 1200 MeV and several angles. Figure 16 shows some of these results with a number of standard deviations (S.D.) varying from 3.0 up to 6.9. The presentation of the results at $T_p = 750$ MeV, $\theta = 40°$ has been changed [6] since the first presentation [11].

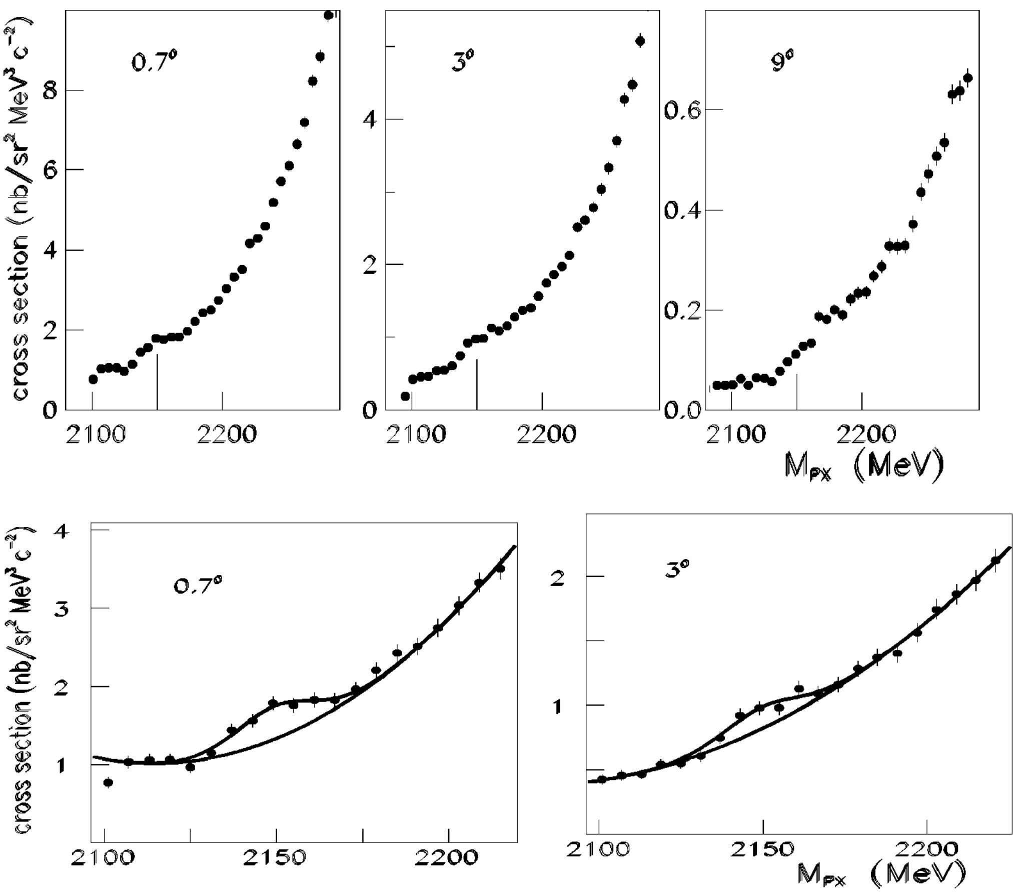

FIG. 14. Cross sections for 2100 MeV incident protons versus M_{pX} dibaryonic mass showing a dibaryonic structure at 2150 MeV.

The same reaction was studied at Los Alamos with polarized protons ($T_p = 800$ MeV) [13]. The analyzing power data showed structures for several M_X close to the dibaryonic masses [11,12] observed previously.

The same situation occurred for a dibaryon around 2190 MeV. It was observed with a good statistical precision using the ^{3}He$(p,d)X$ reaction at Saturne and Los Alamos (same references).

2. The d' resonance

A narrow dibaryon at 2060 MeV, has been advocated for several years. It was deduced [14] from pionic double charge exchange (DCX) reactions on several nuclei from ^{14}C to ^{48}Ca. This narrow dibaryon was supported by a recent result of DCX reaction study on ^{4}He performed at TRIUMF using the CHAOS spectrometer [15]. The existence of the d' resonance was confirmed in a two pion production reaction, namely the $pp \Rightarrow pp\pi^-\pi^+$ reaction performed at ITEP [16] and at CELSIUS using a 750 MeV proton beam [17]. The experiment is similar to the one presented here, except that at Celsius, the energy was lower, the invariant $M_{pp\pi^-}$ mass was reconstructed, and a relatively narrow range of $M_{pp\pi^-}$ mass (2055 ± 25 MeV) was studied. A narrow peak at 2063 MeV (with a statistical significance of four sigmas), was found. This might be the same as the one which appears in our data at 2050 MeV (see Fig. 7). A status report concerning the d' searches in DCX and pp collisions was recently published [18]. In this paper, a table shows a list of various experiments with data analysis in progress. An enhancement at 2060 MeV (with a statistical significance of two sigmas), was observed in the ^{4}He$(\pi^+,\pi^- pp)$ invariant mass search [19], studied at TRIUMF with 115 MeV π^+ beam.

Several theoretical calculations were performed in connection with this result [20–23]. The d' isospin was anticipated as being even, and $J^P = 0^-$ since a very small width ($\Gamma_{\pi NN} \approx 0.5$ MeV) was observed. This leads to the conclusion that the d' cannot decay into two nucleons. The two possibilities of isospin, 0 and 2, were investigated and discussed within the constituent quark model calculation (six quark system) [24] for a possible $J^P = 0^-$ dibaryon at 2065 MeV.

The first assignment of isospin 0, was supported by a QCD string model and three-body calculations and by nonrelativistic Fadeev equations with local potentials [25] (see several references inside). Using the resonating group model, the mass and wave function of a six-quark system of the

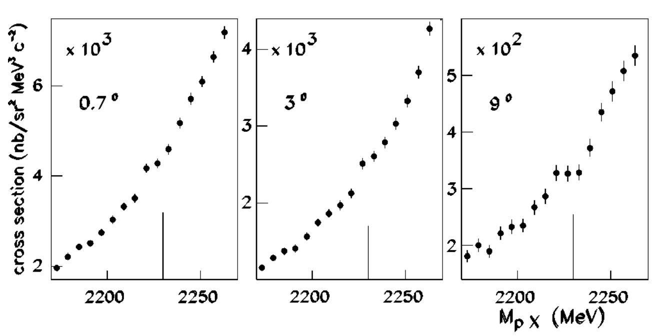

FIG. 15. Cross sections for 2100 MeV incident protons versus M_{pX} dibaryonic mass showing a dibaryonic structure around 2230 MeV (vertical straight lines).

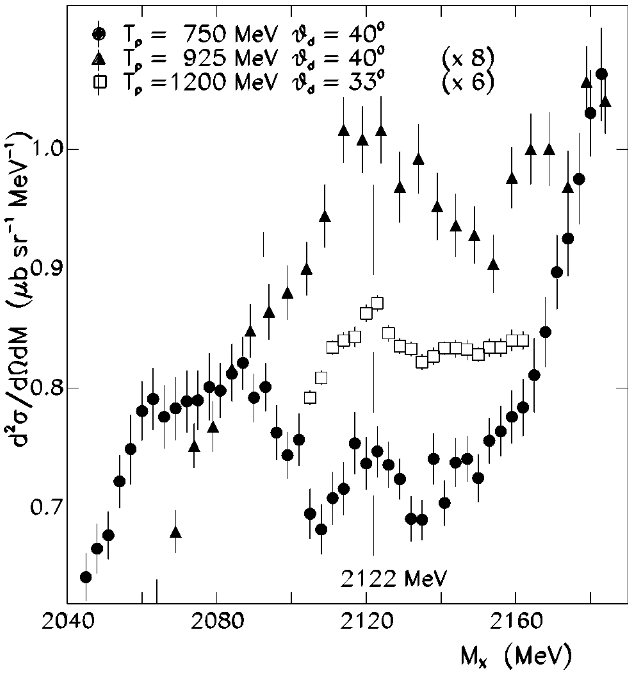

FIG. 16. Missing mass spectra for ^{3}He$(p,d)X$ reaction showing the presence of a narrow dibaryon at M_X=2122 MeV [11,12].

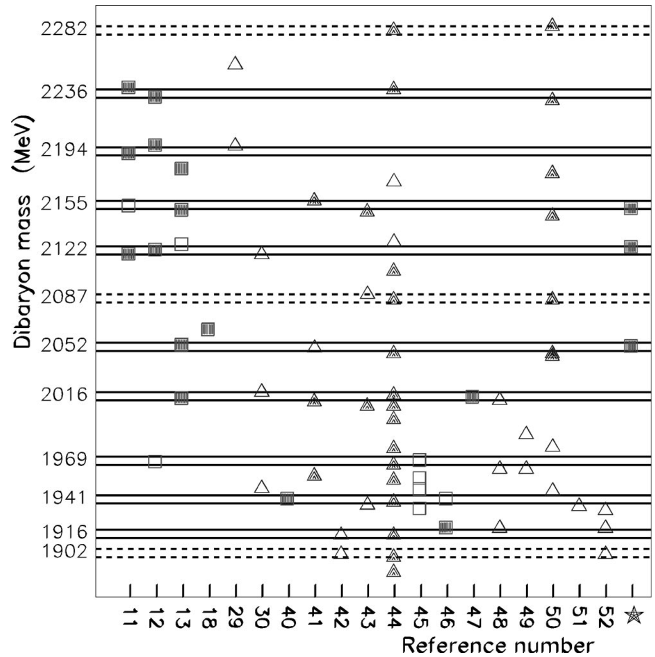

FIG. 17. Masses of experimental narrow structures observed in previous experiments versus the corresponding reference. The last column (⋆) corresponds to the masses observed in this work. (See Refs. [11–13,18,29,30,40–52].)

$d'(J^P=0^-,T=0)$ was recently calculated [26]. Meanwhile isospin 2 was proposed [27], supported by the small experimental width according to relativistic calculations and isobar model with first-order perturbation theory. The same isospin was proposed [28] using a nucleon-Δ interaction based on quark cluster model.

Of course, isospin 0, which is presently preferred to isospin 2 [15], is not excluded by our reaction. However, our observed width for the dibaryon at 2050 MeV ($\sigma\approx 12.6$ MeV) is larger than the reported width of the $d'(\Gamma_{\pi NN}\approx 0.5$ MeV). Our experimental resolution (σ) for M_{pX} or M_{pn}, is estimated as being equal to 3.1 MeV at 0°, and increases with increasing angle. Unless our structure observed at 2050 MeV in M_{pn} invariant mass corresponds to another dibaryon than the d', then the conclusion on the values of spin and isospin for this $d'(J^P=0^-,T=0)$, supported by the assumption of noncoupling with the two-nucleon channel, must be reexamined.

3. $pd\rightarrow\pi^-ppp$ experiment

The invariant $M_{pp\pi^-}$ mass was studied using a 3300 MeV/c deuteron beam [29]. Two narrow enhancements were observed after quasifree processes suppression at masses: 2199±7 and 2258±2 MeV. The first one compared favorably with the mass depicted in Fig. 17 at 2194 MeV. An analysis based on the impulse approximation correctly reproduced the shape of the distributions below the narrow peaks.

4. $pd\rightarrow pnp$ experiment

The M_{np} invariant mass spectra from the $pd\rightarrow pnp$ reaction at 1000 MeV was studied [30]. Narrow dibaryons were extracted in the direct channel at 1950, 2020, and 2120 MeV. The two last masses precisely fit previous assignments (see Fig. 17). The first mass has no counterpart on the same figure, although it is fair to admit that the experimental situation in this mass range is not clear.

5. $pn\rightarrow\pi^-pp$ reaction

The invariant mass of two protons was studied using the $pn\rightarrow\pi^-pp$ reaction [31] at ITEP (1980 MeV/c) protons. No narrow dibaryon was observed in this experiment in the mass region $1890<M_{pp}<2170$ MeV.

6. $\pi^+d\rightarrow pp$ reaction

A precise $\pi^+d\rightarrow pp$ experiment was performed to study an eventual structure in the energy dependence of this reaction [32]. Small steps in pion energy were used from 18 to 44 MeV, which corresponds to $2032<\sqrt{s}<2056$ MeV. This is a very small energy range for dibaryon search (see Fig. 17). Only one level is predicted inside that range, and it is located on the upper side at 2052 MeV. No structure was observed in that experiment.

7. $pp\rightarrow\gamma\gamma pp$ experiment

The theory of this reaction was considered [33,34], since it offers the advantage of allowing the study of narrow dibaryons with masses below the pion emission threshold (2014 MeV) where the probability of parasitic reactions is reduced. This two-photon process is of course experimentally difficult due to the low counting rate. A narrow peak at 1923.5±4.5 MeV with a statistical significance of 8σ was observed [35]. This value is close to 1916 MeV, which is a mass already reported in Fig. 17. However the same reaction was recently studied at CELSIUS [36]. Narrow dibaryons were looked for in the mass range 1900 up to 1960 MeV. The authors concluded that their data presented no indication of a state in the 1917–1923 MeV range. However, if several states do actually exist, separated by a few tens of MeV, the superposition of the corresponding peaks and their mirror peaks, could produce a flat distribution compatible with the results they show in Fig. 3 of their paper, implying a cross section lower than 50 nb.

8. $pp \rightarrow pn\pi^+$ experiment

A precise kinematically complete $pp \rightarrow pn\pi^+$ experiment was performed near threshold [37]. The M_{pn} invariant mass varies between threshold (1878 MeV) and 1891 MeV for the largest incident energy. The aim of the experiment was not the study of dibaryons, and it is clear that such a small range is not suitable for such a study.

9. $\pi^- d \rightarrow \gamma X (X = \pi^0 nn, \pi^- pn)$ experiment

This experiment was performed at TRIUMF [38]. Pions were stopped in D_2 in order to produce $(\pi^- d)$ atoms. A transition from these atoms to neutral $\pi^0 nn$ or $\pi^- pn$ could give a peak in the case of a sufficiently narrow dibaryon. However, no peak was observed in the expected γ ray range of 10 to 20 MeV, that is ± 5 MeV on both sides of 2002 MeV where a possible candidate was previously indicated from the $d(\pi^{\mp}, \pi^{\pm})X$ experiment.

10. $\vec{p}p \rightarrow \pi^- X$ experiment

This experiment was performed at Saturne, in the SPES3 beam line at three energies, 1450, 2100, and 2700 MeV, in order to search for isospin $T=2$ dibaryons in the missing mass data [3,39–52]. Only one structure at 2164 MeV was extracted ($\Gamma_{1/2} = 15$ MeV, S.D.=2.6). Since this mass is close to the $M_\Delta + M_N$ mass, it is difficult to eliminate a threshold effect.

C. Total and differential cross sections and asymmetries for the $\vec{p}p \Rightarrow pp\pi^0$ reaction

Although no enhancement was observed in these observables measured at Saturne [53], a simultaneous analysis of this data and of the results obtained previously from the $np \Rightarrow NN\pi^{\pm}$ reaction lead the authors to conclude that a strong possibility exists for a significant contribution of a $^1D_2$ partial wave in the isoscalar channel near $\sqrt{s} = 2129$ MeV. This energy is the same as our peak mass of 2122 MeV and is within the energy resolution of the pion production experiments. Our $\vec{p}p \rightarrow p\pi^+ X$ reaction allows isospin 0 and 1 (even 2). The same dibaryonic mass was observed previously in the ^{3}He$(p,d)X$ reaction (already mentioned in Sec. IV B 1) in an isovector channel. The fact that the same dibaryonic mass was observed in isospin channels 0 and 1 can be related to isospin degeneracy, predicted by some models which will be discussed further on.

V. ATTEMPT TO DEFINE AN EXPERIMENTAL SET OF NARROW DIBARYONS

Many experiments observed narrow structures in dibaryonic masses and concluded on their genuine existence. However, only some amongst all these results had a statistical precision which allowed them to be conclusive. A part of those precise results was recalled in previous paragraphs. As was already noticed, the weakness of the signatures and their superposition on a large physical background, makes this work difficult. Therefore, we compared all of the results in order to try to increase the confidence we could have on their genuine existence.

In an attempt to define which dibaryonic masses were observed with a reasonable confidence level, we have plotted in Fig. 17 the masses of the narrow structures (vertical axis) reported by the authors whose references are displayed on the horizontal axis. Here the experiments performed with electronics are noted with squares and those from bubble chambers are noted with triangles. Full symbols correspond to data with S.D.$>$3.07 (confidence level $>$99%), and open symbols to data with S.D.$<$3.07. In some cases, the S.D. were not quoted by the authors but estimated from the published data. The experimental masses are not spread but concentrated around some particular values. These values are listed on the vertical scale and are called ''Dibaryon mass.'' The double line corresponds to ± 3 MeV, which can be considered as being an approximate precision for experiments performed with electronics.

VI. ATTEMPT AT AN INTERPRETATION

More general than the study of dibaryons, the stability of exotic bound states of negative pions and neutrons was investigated [54]. Different theoretical papers deal with narrow dibaryons, either their existence, or their decay modes or the consequence of their hypothetical existence on some other observables. One consequence is the possibility of a Bose condensate of dibaryons occuring in nuclear matter [55]. Some works were performed within the chiral soliton model [56]. The consequences of dibaryons on nuclear matter properties, or on the structure of neutron stars [57,58] were considered. The inelastic production cross section of d^* (isoscalar $J^\pi = 3^+$ didelta dibaryon) was calculated [59] and found to be in the μb/sr range, although it was not observed [60] in a $dd \rightarrow dX$ experiment. Its decay width into two nucleons was found to be in MeV's. It is not the aim of the present work to recall the various theoretical works which were devoted to dibaryon studies.

A. The phenomenological mass formula

Here we will present a very simple phenomenological relation, which nonetheless allows us to predict the observed ''experimental masses'' with a surprising accuracy.

The mass formula for two clusters of quarks at the end of a stretched bag was derived some years ago in terms of color magnetic interactions [61]:

$$M = M_0 + M_1[i_1(i_1+1) + i_2(i_2+1) + (1/3)s_1(s_1+1) + (1/3)s_2(s_2+1)], \tag{1}$$

where M_0 and M_1 are parameters deduced from mesonic and baryonic mass spectra and $i_1(i_2)$, $s_1(s_2)$ are isospin and spin of the first and second quark cluster, respectively. We make the assumption that the clusters are $q^2 - q^4$. The spin and isospin values for a diquark (q^2) cluster are 0 or 1 and for a 4 quark cluster (q^4) they are 0, 1, or 2. We consider the two parameters M_0 and M_1 as being free and therefore we will

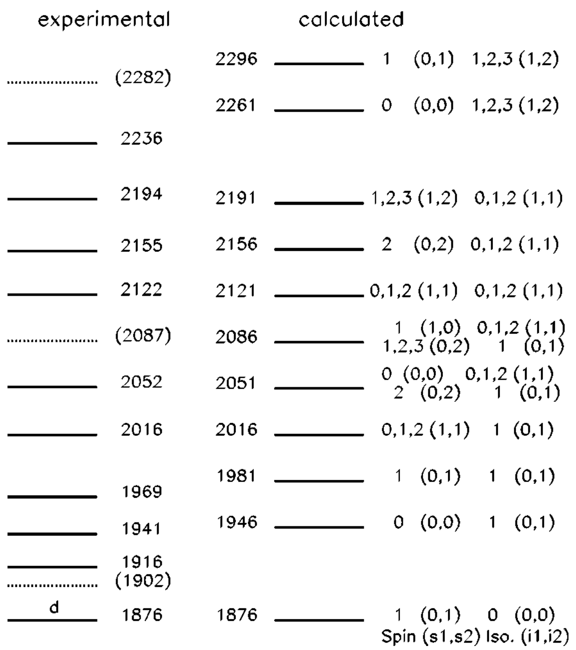

FIG. 18. Experimental masses of narrow dibaryons (left) and masses calculated using the mass formula of Eq. (1). The numbers in parenthesis (right) indicate the two possible spin and isospin values for the two quark clusters.

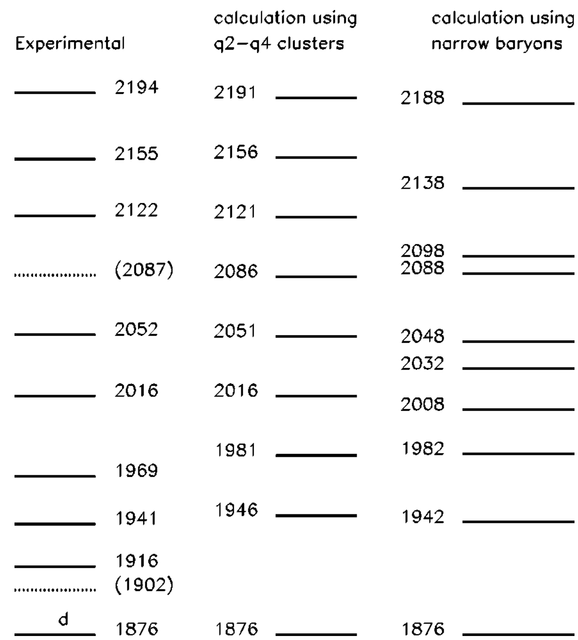

FIG. 19. Masses of narrow dibaryons. From left to right: experimental results, calculated results using the q^2-q^4 clusters mass formula (1) and values found using the narrow baryonic masses.

also consider the formula as a phenomenological one. We first assume that the deuteron mass is obtained when $i_1=i_2=0, s_1=0$ and $s_2=1$ [62], therefore giving the deuteron quantum numbers $S=1, I=0$. In this case $M_d=M_0+(2/3)M_1$. We choose $M_0=1841$ MeV and $M_1=52.5$ MeV, in order to get the deuteron mass and the best agreement for the other masses. These parameters are about 12% lower than the corresponding values reported in [61]. The ratios between our values and those of [61] are 0.86 for M_0 and 0.89 for M_1. Couples of i_1 and i_2 allowing total isospins 0, 1, or 2, have to be considered if $M_X > M_n$ (otherwise total isospin=0 or 1). However, if we restrict ourselves to dibaryonic masses below 2200 MeV, the calculated masses for isospin 2 do not introduce new levels, and the calculated masses for isospin 0 introduce only one additionnal level at 1911 MeV. Such results illustrate the strong degeneracy of the formula. The calculated mass spectra is shown in Fig. 18. All the ''experimental levels'' are reproduced except for those at 1916 and 1902 MeV. From 2000 MeV to 2200 MeV the agreement with ''experimental masses'' is very good, with deviations $\leqslant 1$ MeV. A similar good agreement between calculated masses using the same mass formula and recently observed narrow baryons was reached [1].

Angular distributions are needed to allow experimental spin determinations, for further comparison with the predictions (given in Fig. 18), but the statistical precision has been too low up until now, to allow such studies.

B. The diquark cluster model

A diquark cluster model for any multiquark system $q^k\overline{q^h}$ was developed by Konno *et al.* [63]. Amongst their different assumptions, let us recall the following: '' Two quarks are strongly bound when they are in the same diquark cluster, if they are both in the $1s_{1/2}$ shell.'' The nonstrange dibaryon q^6 consists simply of three such diquarks, where all quarks are u or d. This model predicts the coexistence of broad and narrow resonances. It is a semiphenomenological model since there are eight parameters determined using baryon masses and πd phase shifts [63]. An agreement was found with the broad dibaryon mass spectrum [64].

There were also other calculations based on the diquark model [65] and on the symmetry properties. This theory was applied mainly to exotic mesons or H dibaryons and not to nonstrange low mass dibaryons.

C. Are narrow dibaryons a consequence of narrow baryons recently observed?

Narrow baryons were recently observed at low masses between neutron mass and Δ^0 mass, namely at 1004, 1044, and 1094 MeV [1]. Within the assumption that the narrow dibaryon masses are produced by all combinations of two baryonic masses (using the nucleon mass and the masses of the narrow baryons), we get a level sequence shown in the right part of Fig. 19. The comparison with experimental dibaryons shows an agreement for several masses. Moreover, the level density found is not very different from the experimental one.

VII. CONCLUSION

The $pp \to p\pi^+X(X=n$ or $N\pi)$ reaction was studied at the following three energies: 1520, 1805, and 2100 MeV and at several angles from 0 to 17° lab. In the invariant M_{pX} masses, several narrow dibaryons were observed at 2050, 2122, and 2150 MeV. These masses were compared to experimentally observed narrow dibaryons in previous experiments and were also compared to some phenomenological mass formulas. The agreement with narrow dibaryon masses observed in previous experiments is good.

The agreement with the phenomenological mass formula is noteworthy. When narrow *baryonic* masses are used to reconstruct the *dibaryonic* masses, the agreement is fairly good. The importance of such agreement lies in the simplicity of these approaches.

These results were also compared with the diquark model. We have found that the theoretical outline here is not as convincing in view of the observations as it was in the case of baryons.

During the data analysis a strongly excited broad structure was observed at 2300 MeV for 2100 MeV protons (not shown in the figures) and at 2270 MeV for 1805 MeV protons. These broad structures were associated with $\Delta^{++}\Delta^{0}$ dynamic resonant states and not with genuine dibaryons. Another broad structure was observed at 2170 MeV, and was associated with the $\Delta^{++}n$ dynamic resonant state.

At this time when the true existence of these narrow structures is becoming more and more clear, in spite of experimental difficulties due to the weakness of the signals, the following two questions arise .

Which conditions provoke the excitation of a specific dibaryonic mass in comparison to other dibaryonic masses in experiments where the range studied allows the observation of several dibaryons?

What is the common origin of narrow *baryons* and narrow *dibaryons* observed nowadays?

Some ideas were proposed. They have to be confirmed and a complete explanation has still to be made. All results concerning narrow dibaryons will be very useful for the study of color confinement at large distances.

ACKNOWLEDGMENTS

We wish to thank Dr. Marion Mac Cormick and Natalie Lutz for help in writing the English version of our paper.

[1] B. Tatischeff, J. Yonnet, N. Willis, M. Boivin, M. P. Comets, P. Courtat, R. Gacougnolle, Y. Le Bornec, E. Loireleux, and F. Reide, Phys. Rev. Lett. **79**, 601 (1997).
[2] J. Yonnet, B. Tatischeff, N. Willis, M. Boivin, M. P. Comets, P. Courtat, R. Gacougnolle, Y. Le Bornec, E. Loireleux, and F. Reide, Nucl. Phys. **A637**, 63 (1998).
[3] M. P. Combes-Comets *et al.*, Phys. Rev. C **43**, 973 (1991).
[4] M. P. Combes-Comets, M. Boivin, Y. Le Bornec, E. Loireleux, B. Tatischeff, and N. Willis, IPN, Orsay Report No. IPNO DRE 88-41 (unpublished).
[5] B. Tatischeff, in Proceedings of the XIIth International Seminar on High Energy Physics Problems, Dubna, 1994.
[6] B. Tatischeff, M. P. Comets, Y. Le Bornec, and N. Willis, in *Proceedings of the Xth International Seminar on High Energy Physics Problems*, Dubna, 1990, edited by A. M. Baldin, V. V. Burov, and L. P. Kaptari (World Scientific, Singapore, 1990), p. 177.
[7] D. Albers *et al.*, Phys. Rev. Lett. **78**, 1652 (1997).
[8] H. Shimizu *et al.*, Phys. Rev. C **42**, R483 (1990).
[9] Y. Kobayashi *et al.*, Nucl. Phys. **A569**, 791 (1994).
[10] R. Beurtey *et al.*, Phys. Lett. B **293**, 27 (1992).
[11] B. Tatischeff *et al.*, Phys. Rev. C **36**, 1995 (1987).
[12] B. Tatischeff *et al.*, Europhys. Lett. **4**, 671 (1987); Z. Phys. A **328**, 147 (1987).
[13] L. Santi *et al.*, Phys. Rev. C **38**, 2466 (1988).
[14] R. Bilger, H. A. Clement, and M. G. Schepkin, Phys. Rev. Lett. **71**, 42 (1993); **72**, 2972 (1994); K. Föhl *et al.*, *ibid.* **79**, 3849 (1997).
[15] J. Gräter *et al.*, Phys. Lett. B **420**, 37 (1998).
[16] L. S. Vorob'ev *et al.*, JETP Lett. **59**, 77 (1994).
[17] W. Brodowski *et al.*, Z. Phys. A **355**, 5 (1996).
[18] R. Bilger, Nucl. Phys. **A629**, 141c (1998).
[19] R. Meier *et al.*, in *Proceedings of the 14th International Conference on Particles and Nuclei* (World Scientific, Singapore, 1997), p. 368.
[20] A. Bobyk, A. Faessler, and A. Kaminski, J. Phys. G **23**, 375 (1997).
[21] R. Bilger, H. Clement, Th. Czarnecki, K. Fohl, B. Martemyanov, M. Schepkin, L. Vorobyev, and G. J. Wagner, Nucl. Phys. **A596**, 586 (1996).
[22] H. Garcilazo, J. Phys. G **23**, 1101 (1997).
[23] K. Itonaga, A. J. Buchmann, G. Wagner, and A. Faessler, Nucl. Phys. **A609**, 422 (1996).
[24] G. Wagner, L. Ya. Glozman, A. J. Buchmann, and A. Faessler, Nucl. Phys. **A594**, 263 (1995).
[25] H. Garcilazo, Phys. Rev. C **56**, 1751 (1997).
[26] A. J. Buchmann, G. Wagner, and A. Faessler, Phys. Rev. C **57**, 3340 (1998).
[27] H. Garcilazo and L. Mathelitsch, Phys. Rev. Lett. **72**, 2971 (1994).
[28] E. Moro, A. Valcarce, H. Garcilazo, and F. Fernández, Phys. Rev. C **54**, 2085 (1996); A. Valcarce, H. Garcilazo, and F. Fernández, *ibid.* **52**, 539 (1995).
[29] A. Deloff and T. Siemiarczuk, Z. Phys. A **353**, 121 (1995).
[30] A. Deloff and T. Siemiarczuk, Nucl. Phys. **A555**, 659 (1993).
[31] B. M. Abramov *et al.*, Z. Phys. C **69**, 409 (1996).
[32] E. A. Pasyuk *et al.*, Phys. Rev. C **55**, 1026 (1997).
[33] S. B. Gerasimov, S. N. Ershov, and A. S. Khrykin, Phys. At. Nucl. **58**, 844 (1995).
[34] V. L. Lyuboshitz and M. I. Podgoretsky, Phys. At. Nucl. **59**, 262 (1996).
[35] V. M. Abazov *et al.*, JINR report E1-96-104.
[36] H. Calén *et al.*, Phys. Lett. B **427**, 248 (1998).
[37] J. G. Hardie *et al.*, Phys. Rev. C **56**, 20 (1997).
[38] S. Stanislaus, D. S. Armstrong, D. F. Measday, P. Weber, and M. Harston, Phys. Lett. B **219**, 237 (1989).
[39] N. Willis *et al.*, Phys. Lett. B **229**, 33 (1989).
[40] B. Tatischeff *et al.*, Phys. Rev. C **45**, 2005 (1992).
[41] O. B. Abdinov, A. A. Baireamov, Yu. A. Boudagov, Yu. Ph. Lomakin, A. A. Mailov, V. B. Fliagin, and Yu. N. Khargeev, JINR report P1-88-102 (in Russian).
[42] N. Angelov *et al.*, JINR report P1-88-905; S. A. Azimov, K. G. Gulamov, S. O. Edgorov, M. Yu. Kratenko, S. L. Lutpulleev, K. T. Turdeliev, A. A. Yuldashev, and B. S. Yuldashev, 60-88 HEP (Tashkent report).
[43] V. V. Glagolev *et al.*, Yad. Fiz. **51**, 736 (1990) [Sov. J. Nucl. Phys. **51**, 467 (1990)].
[44] Yu. A. Troyan and V. N. Pechenov, Sov. J. Nucl. Phys. **56**, 191 (1993) (in Russian).

[45] V. V. Avdeichikov *et al.*, Yad. Fiz. **54**, 111 (1991) [Sov. J. Nucl. Phys. **54**, 67 (1991)]; Yu. A. Troyan *et al.*, *ibid.* **54**, 1301 (1991) [**54**, 792 (1991)].
[46] V. B. Ganenko, V. A. Gushchin, Yu. V. Zhebrovskii, Yu. A. Kasatkin, L. Ya. Kolesnikov, S. I. Nagornyi, V. D. Ovchinnik, A. L. Rubashkin, P. V. Sorokin, and A. A. Zayats, Pis'ma Zh. Eksp. Teor. Fiz. **50**, 220 (1989) [JETP Lett. **50**, 224 (1989)].
[47] B. Bock *et al.*, Nucl. Phys. **A459**, 573 (1986).
[48] L. A. Didenko *et al.*, JINR report E1-91-329; E1-91-323.
[49] O. B. Abdinov, A. A. Baireamov, Yu. A. Boudagov, A. M. Dvornik, Yu. Ph. Lomakin, A. A. Mailov, V. B. Fliagin, and Yu. N. Khargeev, JINR Rapid Communications **A15**, 34 (1986).
[50] C. Besliu, L. Popa, and V. Popa, J. Phys. G **18**, 807 (1992).
[51] C. Besliu *et al.*, JINR report, D1-85-433 (in Russian).
[52] S. O. Edogorov *et al.*, FTI report 141-91, FVE Tashkent.
[53] G. Rappenecker *et al.*, Nucl. Phys. **A590**, 763 (1995).
[54] H. Garcilazo, Phys. Rev. C **52**, 1126 (1995).
[55] A. Faessler, A. J. Buchmann, M. I. Krivoruchenko, and B. V. Martemyanov, Phys. Lett. B **391**, 255 (1997); A. Faessler, A. J. Buchmann, M. I. Krivoruchenko, and B. V. Martemyanov, J. Phys. G **24**, 791 (1998).
[56] V. B. Kopeliovich, Phys. At. Nucl. **58**, 1327 (1995).
[57] A. Faessler, A. J. Buchmann, and H. I. Krivoruchenko, Phys. Rev. C **56**, 1576 (1997).
[58] N. K. Glendenning and J. Schaffner-Bielich, Phys. Rev. C **58**, 1298 (1998).
[59] Chun Wa Wong, Phys. Rev. C **57**, 1962 (1998).
[60] M. P. Combes *et al.*, Nucl. Phys. **A431**, 703 (1984).
[61] P. J. Mulders, A. T. Aerts, and J. J. de Swart, Phys. Rev. D **21**, 2653 (1980); **19**, 2635 (1979); Phys. Rev. Lett. **40**, 1543 (1978).
[62] The justification to include the deuteron in that quark clusters systematics is that its short range part wave function can be considered as a six-quark cluster.
[63] N. Konno, H. Nakamura, and H. Noya, Phys. Rev. D **35**, 239 (1987); **37**, 154 (1988); Y. Uehara, N. Konno, H. Nakamura, and H. Noya, Nucl. Phys. **A606**, 357 (1996).
[64] A. Yokosawa, in *Proceedings of Sixth International Symposium on Polarization Phenomena in Nuclear Physics*, Osaka, 1985, edited by M. Kondo *et al.* [J. Phys. Soc. Jpn. **55**, 251 (1986)].
[65] D. B. Lichtenberg, R. Roncaglia, and E. Predazzi, J. Phys. G **23**, 865 (1997).